Eur. Phys. J. Special Topics **158**, 7–14 (2008)

DOI: 10.1140/epjst/e2008-00646-6

THE EUROPEAN PHYSICAL JOURNAL SPECIAL TOPICS

Quasistatic and dynamic functional properties of thin superelastic NiTi wires

L. Heller[1,2,a], A. Kujawa[1], P. Šittner[1], M. Landa[2], P. Sedlák[2], and J. Pilch[1]

[1] Institute of Physics ASCR, v.v.i., Na Slovance 2, Prague 18221, Czech Republic
[2] Institute of Thermomechanics ASCR, v.v.i., Dolejskova 5, Prague 18200, Czech Republic

Abstract. 2D/3D structures made from thin NiTi wires (d $< 100\,\mu$m) are currently considered for engineering applications in textile, medical or robotics fields. The development of such novel applications requires the knowledge of the thermomechanical behaviour of NiTi ultra thin wires in tension, torsion bending and combined loads, which might differ from that of thicker wires due to influence of texture, cold work and higher aspect ratio. To deal with this challenge, a new experimental testing approach presented in this paper has been developed. It includes thermomechanical tensile testing, combined tension-torsion testing and forced tensile vibrational testing realized on self-made testing rigs equipped with Peltier furnaces and in-situ electric measurement systems. The collected experimental datasets provide a basis upon which FEM implementable SMA models describing functional thermomechanical behaviours of 2D/3D NiTi wire structures (quasistatic and dynamic) are presently being constructed

1 Introduction

2D/3D structures made from thin NiTi wires (d $< 100\,\mu$m) using conventional textile production methods such as weaving, knitting and braiding should benefit from the unique functional properties of shape memory alloys. The knowledge of the thermomechanical behaviour of thin NiTi wires is crucial in the stage of modelling and design of such novel structures. First, since the material state of the thin NiTi wires is different from that of the bulk NiTi wires (texture, cold work etc.), their tensile properties cannot be obtained simply by scaling down the results measured on thicker wires but have to be determined experimentally. Second, since the generally shape set thin NiTi wires in 2D/3D structures deform by combined tension-torsion-bending, the responses of the NiTi wires to such general loading conditions have to be investigated and known. Third, since many of the considered NiTi textile applications in fact attempt to utilize the unique damping capabilities of NiTi, dynamical and fatigue behaviour of the thin wires needs to be investigated. New experimental testing approaches developed with the aim to deal with the above introduced challenges are briefly described in this paper and selected results are presented and discussed.

2 Thin NiTi wires

Presently, wide range of thin superelastic and actuator NiTi wires (20–100 μm) is available from SMA providers. The experimental results discussed in this paper concern the superelastic NiTi wires provided by Fort Wayne Metals – FWM (d $= 50, 75, 100\,\mu$m), Memory Metalle – MM

[a] e-mail: heller@fzu.cz

Table 1. Selected identified mechanical parameters relative to different NiTi wires.

wire	R_s °C	R_f °C	M_s °C	M_f °C	A_s °C	A_f °C	E^A GPa	E^M GPa	σ^{tr} MPa	$\epsilon^{tr}_{A\text{-}M}$ %	$\epsilon^{tr}_{A\text{-}R}$ %	σ^{UTS} MPa
MM	12	10	-	-	-	-	72	33	600	6,3	0,6	1780
SG	30	24	-	-	-	-	49,4	21,6	490	4,7	0,4	1600

wire	σ^Y MPa	ϵ^f %	Δh^σ MPa	ϵ_{ac} %	$\Delta\sigma^{tr}_{ac}$ MPa	Δh^σ_{ac} MPa	M'_s °C	A'_f °C	$s_{A\text{-}R}$ MPa/°C	$s_{A\text{-}M}$ MPa/°C	σ^{re} MPa
MM	1520	16	320	0,04	13	31	−110	−30	17	4,7	180
SG	1387	13,3	410	1,36	49	51	−52	0	18,1	6,6	-

(d = 25, 50 μm) and SAES Getters - SG (d = 100 μm). The analysis of thermomechanical properties of thin NiTi wires have shown somehow different results in comparison to thicker wires [1]. These differences are caused by a very high degree of cold work (the order of tens of percents) given during the final stages of the wire drawing process. The highly textured microstructure consisting of nanosized grains provides the higher strength, wide superelastic window [1], better cyclic stability and peculiar torsional properties of the thin NiTi wires dealt with in this paper. The functional properties of superelastic NiTi wires are due to chemical composition, cold work given during the wire drawing and final heat treatment (shape setting). While developing the textile applications, large quantities of the NiTi wires are used. Hence, there is a need to carefully compare functional properties of various superelastic wires supplied by different providers. The unique feature of the SMA technology is that the parameters of the final heat treatment defining in large extent the superelastic behavior of the NiTi wires can be decided by the user [2].

In case of textile processing of annealed superelastic NiTi wires, straight annealing (respooling the wire through a long tubular furnace heated to 500°C under constant preload) performed at the SMA producer side guaranties that the wire supplied on one spool features the same functional properties all over its length. In case of wire supplied on more spools, however, its functional properties needs to be evaluated separately. To describe functional thermomechanical behavior of NiTi wire, it is not sufficient just to measure Ms and Mf temperatures and use them as input for SMA material model. Due to the complexity of SMA functional behaviors, a set of material parameters evaluated consistently using standard testing procedures as well as SMA model taking them as material input are needed. Since these have not been agreed yet in the SMA research community, the first goal of this work was define the material parameters and associated testing procedures and the second goal to develop the SMA model [3] in parallel. The general thermomechanical behavior of a 2D/3D NiTi wire structure is then predicted by a finite element model (FEM) which uses the SMA model for predicting the general loading responses of the NiTi wires. This report focuses the first experimental goal.

3 Quasistatic tensile thermomechanical loads

In order to be able to characterize the functional behavior of NiTi wires, we decided to specify the testing procedures and set of material parameters only for the quasistatic tensile thermomechanical behaviors and utilized these for the modeling of the combined load responses of the wires [3]. Several testing procedures and sets of material parameters have been tried [1]. Finally, it was decided to use a set of 23 material parameters (Table 1, Figs. 1 and 2) divided into four groups: 6 thermal, 9 mechanical, 3 cyclic and 5 thermomechanical parameters.

The first group involves 6 thermal parameters: the martensite (R-phase, austenite) start and finish temperatures (M_s/M_f, R_s/R_f, A_s/A_f, see Fig. 1(c)), second group 9 mechanical parameters (determined from the one tensile test until rupture and one complete superelastic cycle at room temperature (RT), see Fig. 1(a)) includes the Young's moduli of the austenite and martensite phases (E^A/E^M), transformation stress (σ^{tr}), maximum recoverable transformation strain for A-M and A-R transformations ($\epsilon^{tr}_{A\text{-}M}/\epsilon^{tr}_{A\text{-}R}$), ultimate tensile strength (σ^{UTS}), yield stress for plasticity (σ^Y), strain at failure (ϵ^f) and pseudoelastic stress hysteresis (Δh^σ). Cyclic

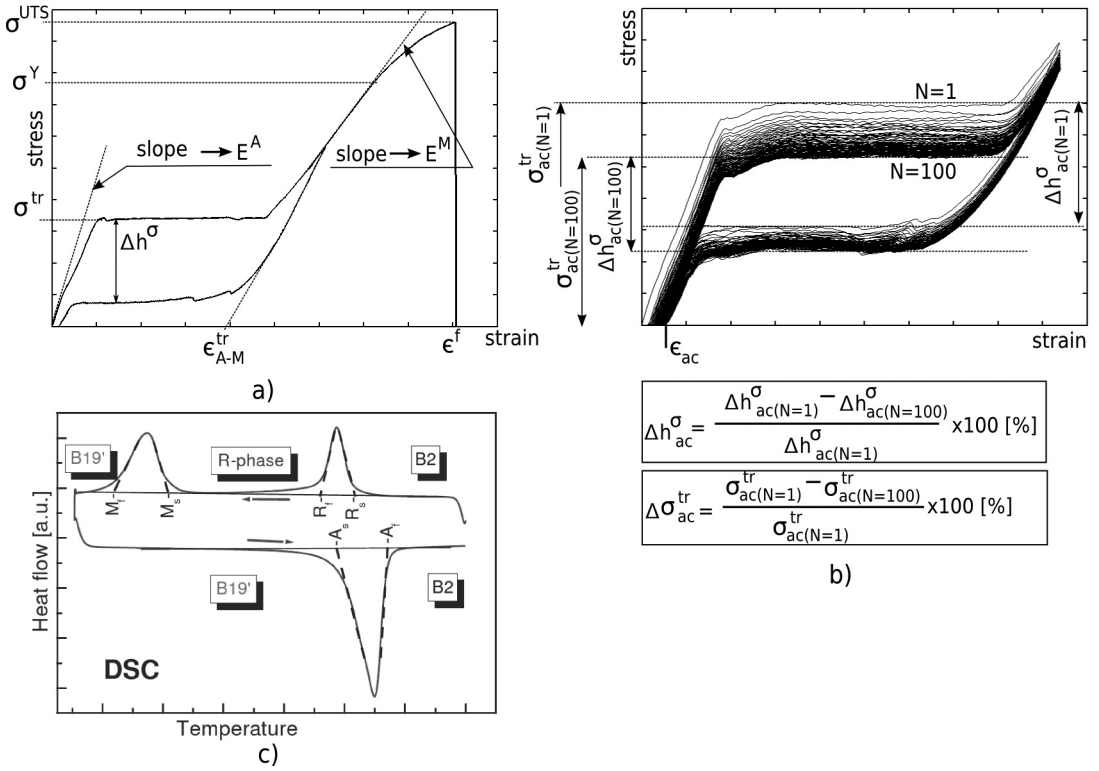

Fig. 1. Material parameters obtained from: a) one tensile test until rupture and one complete superelastic cycle at room temperature (RT), b) cyclic tensile test at RT (100 complete superelastic cycles), c) DSC measurement.

parameters (3) describe the stabilisation of mechanical properties which typically occurs during first hundred tensile superelastic cycles (see Fig. 1(b)): the accumulated non-recovered strain (ϵ_{ac}), cyclic accumulated transformation stress change ($\Delta\sigma^{tr}_{ac}$), cyclic accumulated hysteresis change (Δh^{σ}_{ac}). Finally, 5 thermomechanical parameters are needed to capture the thermomechanical responses: effective martensite start and austenite finish temperatures (M'_s/A'_f), temperature dependences of transformation stresses for A-R and A-M transitions ($s_{A\text{-}R}/s_{A\text{-}M}$) and martensite reorientation stress (σ^{re}). This last group of parameters must be determined from two basic test sets – the complete superelastic tensile cycle tests at different temperatures (Fig. 2(a)) and the thermal cycle tests at different constant stresses (Fig. 2(b)). The identification of the start and the end of the deformation/transformation processes in these tests is beneficially assisted by the in-situ measurement of electrical resistivity [5] as also shown in figures 2(a) and (b).

The measured data are used to construct the non-equilibrium stress-temperature diagram (Fig. 2(c)) [6] summarizing in a compact graphical form the essential information needed to describe the thermomechanical behaviors of the wires. 23 parameters seems to be a large number, particularly taking into account that, from the modelling point of view [3], it is essential that only minimum number of material parameters is used. The parameters, however, must identify and distinguish the activity of all deformation/transformation processes (considered in the modeling) taking place in the thermomechanically loaded NiTi wires (i.e. forward/reverse martensitic and R-phase transformation and reorientation processes in martensite and R-phase). A dedicated paper introducing the parameterization of the thermomechanical behavior of superelastic SMA wires and associated testing procedures in detail will be published separately [4].

The actual values of material parameters measured on superelastic wires MM100 μm and SG100 μm both annealed at 450°C/30 min on air are compared in Table 1. Since the annealing conditions and diameter were the same, the results reveal the differences in functional

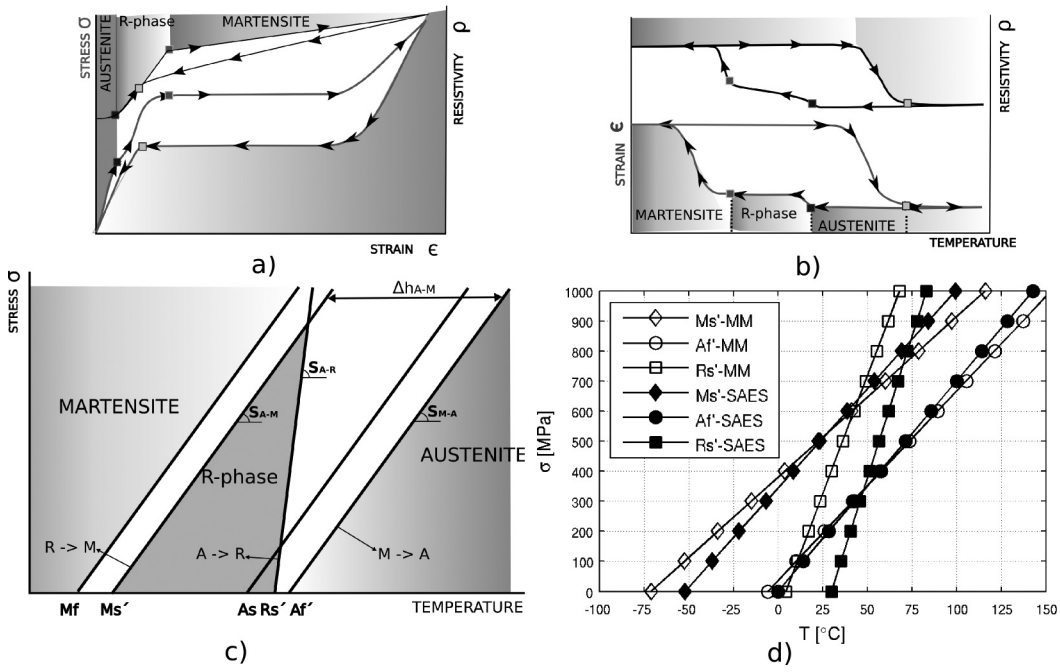

Fig. 2. Testing procedures to evaluate thermomechanical parameters of superelastic NiTi wires (see text): a) tensile cyclic test at constant temperature with in-situ resistivity measurement, b) thermal cycle at constant stress with in-situ resistivity measurement, c) construction of the non-equilibrium stress-temperature phase diagram from multiple mechanical and thermal tests, d) A-M, M-A and R-M transformation lines measured for MM100 μm and SG100 μm.

behaviours of the wires due to the chemical composition and wire drawing process. The identified non-equilibrium stress-temperature phase diagrams clearly show differences in the temperature hysteresis as well as in the temperature dependences of transformation stress. The differences in selected mechanical parameters (Tab. 1) concern mainly the cyclic properties being crucial from the design point of view. It is essential to point out that the set of 23 material parameters allows us not only to select a proper wire for proper application but mainly evaluate the effect of wire drawing and/or heat treatment on the functional properties of the NiTi wires.

In order to provide comprehensive experimental information for confrontation with modeling, we attempted to plot so called transformation strain surface on top of the stress-temperature space with the aim to provide complete information on the actual inelastic strains recorded after a monotonous thermomechanical loadings. Such surface is a model inspired approximation. It can be plot both for the forward and reverse transformations. It assumes uniqueness of the transformation strain for a given stress-temperature state representing the current monotonously growing (decreasing) driving force, whatever is the stress-temperature path.

To construct the transformation strain surface for the straight annealed FWM 50 μm NiTi wire (Fig. 3(a)), complete superelastic tensile cycles at several constant temperatures and the thermal cycles at several constant pre-stresses were used. The measured data are then approximated by a surface and confronted with modeling predictions for the inelastic strains [3]. Although there are differences between the inelastic strains observed in equivalent thermal and mechanical loads, the results (Fig. 3(a)) confirm the usefulness and applicability of the approach. Of course the surface changes, if one allows for non-monotonous variation of the driving force due to the hysteresis, this however can be accounted for by the modeling. In a similar fashion, an electrical resistivity surface was constructed on top of the stress-temperature space (Fig. 3(b)). This surface was found very useful as well, particularly since it allows to determine the stress-temperature regions where the R-phase transformation/reorientation processes associated with only small inelastic strains become active(note the increase of resistivity at low stresses and temperatures in figure 3(b)).

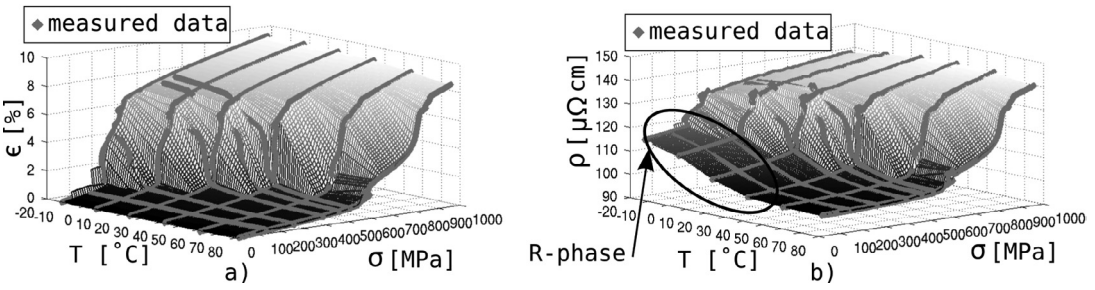

Fig. 3. Experimentally determined transformation strain a) and resistivity b) surfaces corresponding to forward transformation.

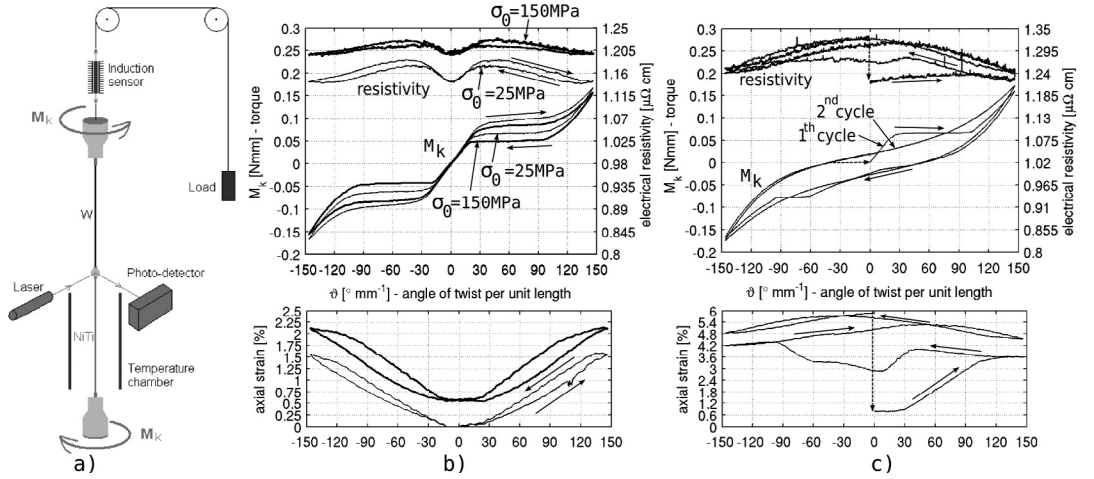

Fig. 4. Combined tension-torsion testing of NiTi wires (FWM 100 μm): a) sketch of the tension-torsion universal tester ATTUT, b) experimental results for tensile prestress 25 MPa and 150 MPa and c) 250 MPa at room temperature.

In summary, the set of 23 material parameters and associated testing procedures were used as a figure of merit for: i) comparing functional behaviors of various superelastic NiTi wires for textile applications, ii) evaluating the effect wire drawing and/or heat treatments on functional properties of the wires, and iii) together with the in parallel developed SMA model [3] for prediction of general uniaxial thermomechanical functional behaviors of the NiTi wires in tension.

4 Quasistatic combined tension-torsion loads

Since the superelastic NiTi wires integrated in the textile experience combined tension-torsion-bending loading mode regardless whether they were shape set into straight or wavy form, we need to investigate at least their combined tension-torsion and bending responses. The SMA model [3] could be extended to treat the more complex stress-strain responses of NiTi wires only based on the representative experimental results. A dedicated experimental equipment ATTUT (Fig. 4(a)) has been designed and built for the purpose of tension-torsion investigations. The device working on a comparator principle allows to evaluate the thermomechanical responses of the $\sim 100\,\mu$m thin NiTi wires upon an applied constant tension load and controlled rate of torque and temperature. Selected experimental results (FWM 100 μm superelastic NiTi wire) in combined tension (pre-stress 25 MPa, 150 MPa, 250 MPa) and torsion at room temperature are shown in figures 4(b) and (c). The progress of the stress induced martensitic transformation is clearly evidenced by the superelastic plateau shaped torque-twist angle curve in figure 4(b). Note

that the maximum reached normalized twist angle $\vartheta = 100°$ per 1 mm length of the 50 mm long and d = 100 μm thin wire corresponds to ~ 21 turns. The end of the superelastic plateau on the torque-twist angle curve thus corresponds to the engineering shear strains ($\gamma = \frac{d}{2}\vartheta$) on the wire surface as large as 5% which is a very large value for a metal. Due to the strong tension-torsion coupling characteristic for SMA functional responses [7], the wire shows significant reversible axial strain change driven by the torsional loading under constant axial stress. Note, however, the dramatic change of the stress-strain response with increasing value of the tensile prestress – i) in torsion, the superelastic response (prestress $<$ 150 MPa) changes into pseudoplastic (prestress $>$ 250 MPa) and ii) the cyclic variation of axial strain accompanying the twisting of the wire changes from positive (1.5%) at tensile prestress 150 MPa to negative (-1, 2%) at 250 MPa. Since the applied pre-stress in tension contributes to the entire multiaxial driving force, its increasing value leads to decrease of the plateau observed on the torque-torsion curve (25 MPa $\rightarrow$ 150 MPa), to the large axial strains and ultimately to the loss of the superelasticity during cyclic torsional loading at all (150 MPa $\rightarrow$ 250 MPa).

The in-situ measured evolution of the electrical resistivity (Fig. 4(b) and (c)) can not be interpreted as easily as reported above for the tensile tests (Fig 2(b)). Nevertheless, even in combined tension-torsion, the initial resistivity increase is probably related to the stress-induced austenite to R-phase transformation [5]. On the other hand, when the stress induced martensitic transformation occurs (Fig. 4(b)), electrical resistivity decreases (remains nearly constant with increasing tensile prestress) in contrast to what observed in tensile tests [5].

In the test at tensile prestress 250 MPa (Fig. 4(c)), the superelastic recovery of inelastic strains upon torsional unloading (only partial unloading since the wire is still exposed to tensile stress) does not occur. It is evident that significant volume fraction of the martensite phase (corresponding to axial strain 6%) remains in the wire after the torsional unloading. As a result of the constant pre-stress, next torsional loading and unloading is accompanied by further increasing volume fraction of the frozen in martensite phase and hence increasing axial strain leading to some kind of 'rachetting axial strain response', which however quickly stabilizes. Upon complete unloading (both torque and axial prestress), the initial values of torsional and axial strains as well as the initial value of electrical resistivity were restored proving that no plastic deformation was involved in the process at all.

The reported combined tension-torsion responses are rather complex, nevertheless, their knowledge is essential for understanding the functional behaviors of 2D/3D NiTi shape set structures and textiles. The gathered experimental datasets are used to further develop the SMA model [3] so it is capable to treat the responses of shape set NiTi wire structures in which combined tension-torsion stress states are expected (e.g. superelastic helical springs, braided tubular NiTi wire structures or twisted NiTi yarns).

5 Dynamic tensile loads

The superelastic damping capacity (ability to attenuate mechanical vibrations due to the energy dissipation stemming from the superelastic hysteresis) is commonly referred to as an additional SMA property promising for engineering applications [8,9], although really developed applications are scarce. There are two main factors limiting the successful exploitation of superelastic damping: i) the amplitude of vibrations has to be sufficiently large to induce significant progress of martensitic transformation and thus phase fraction change and hysteresis [8], ii) the poor fatigue properties of the NiTi wires loaded in tension [10] makes it problematic for damping of forced vibrations. Since these two issues are not of primary importance for seismic applications, superelastic damping has mainly found applications in seismic protection.

In order to explore the potential superelastic damping applications of NiTi textiles, investigation of the dynamic behaviour of thin superelastic NiTi wires has been started. A dedicated vibrational tester AVUT (Fig. 5(a)) allowing to measure the static and dynamic components of the sinusoidally varying tensile force and the displacement of its extremity was designed and built. Figure 5 shows selected results of experimental investigations focusing the superelastic damping capacity of the straight annealed NiTi wires (FWM, d = 100 μm) at room

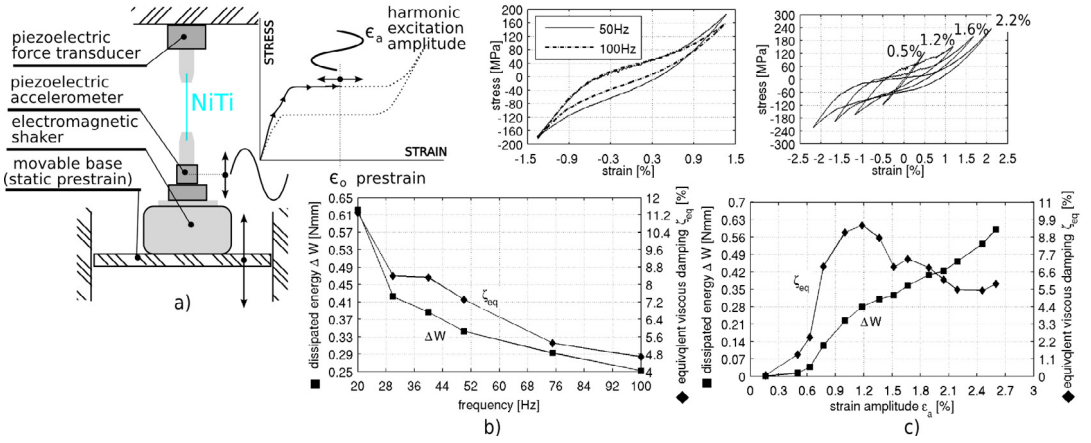

Fig. 5. Dynamic tensile testing of NiTi wires (FWM 100 μm): a) sketch of the vibrational tester AVUT, b) frequency dependence of damping and example of stress-strain loop for 1.2% strain amplitude and frequencies 50 Hz and 100 Hz, c) strain amplitude dependences of damping and example of stress-strain loops at 50 Hz.

temperature. Besides of the evaluation of the dissipated energy, ΔW, as the area of the force-displacement curve, the damping capacity was also evaluated as the equivalent viscous damping $\zeta_{eq} = \frac{1}{4\pi} \frac{\Delta W}{E_{kmax}}$ (measures the damping efficiency taking into account the amount of introduced energy needed to dissipate a given energy ΔW through the presence of maximum kinetic energy E_{kmax}).

From the first set of experiments with cycling at constant strain amplitude and variable frequencies (Fig. 4b), it was found that both the dissipated energy ΔW and equivalent viscous damping ζ_{eq} significantly decreases with increasing frequency from 20 Hz to 100 Hz limiting thus the damping capacity of the wire at higher frequencies. Compare the different hysteresis loop areas measured in the tests run at 50 Hz and 100 Hz (Fig. 5(b)). Nevertheless, the damping coefficient $\zeta_{eq} = 4.8\%$ measured at frequency 100 Hz is still quite a large value compared to other high damping materials capable of recoverable deformation up to comparable strain amplitudes (rubber$\sim 30\%$, epoxy$\sim 1.5\%$, Al$\sim 0.9\%$ [9]).

Second set of experiments (Fig. 5(c)) was performed at the constant frequency 50 Hz and prestrain 2.25% but variable strain amplitude (0.15%–3%). The damping capacity was found to depend on the vibration strain amplitude in a complex manner (Fig. 5(c)). There is a rapid increase of the damping capacity (both ΔW and ζ_{eq}) with increasing strain amplitudes in the range 0.6%–1.2% suggesting that a minimum dynamic strain amplitude must be reached to fully activate the progress of the martensitic transformation during cyclic loading. Once this is fulfilled, the dissipated energy ΔW increases with strain amplitude linearly with much lower rate. The viscous damping coefficient ζ_{eq}, however, shows a local maximum (Fig. 5(c)) at strain amplitude 1.2% and than decreases up to the strain amplitude 2.5%.

We found out that these phenomena can be rationalized considering the effect of strain rate on the periodical heat generation/absorption occurring during the superelastic cycle [10]. The strain rate increases with both the frequency (Fig. 5(b)) and the strain amplitude (Fig. 5(c)) and when it reaches a rate for which the latent heat exchange is not efficiently absorbed by the convection into the surrounding space, it reduces the damping capacity of the wire.

It thus comes out of the present investigations that there is a third factor limiting significantly the superelastic damping capacity and this is the periodical heat generation/absorption accompanying superelasticity. In the case of the thin NiTi wires, this third limiting factor is partly eliminated by a high surface/volume ratio improving the latent heat dissipation. Because of this, tensile cyclic of thin NiTi wires with large strain amplitudes is realizable even at higher frequencies reaching 100 Hz.

6 Conclusion

Experimental approaches towards characterization of thin superelastic NiTi wires for textile applications including selected results were presented and discussed.

A set of 23 material parameters and associated testing procedures was specified and used systematically to characterize the quasistatic tensile termomechanical functional responses of thin superelastic NiTi wires. The parameters served as figure of merit for selection of wires for particular applications, evaluation of the wire drawing and/or heat treatment effects on functional properties as well as input into SMA model predicting the NiTi wire responses for application design.

Dedicated experimental device for quasistatic combined tension-torsion testing was used to gather experimental data necessary for further development of the SMA model so it can treat the behaviors of the NiTi wires under general loading conditions (combined tension-torsion-bending conditions existing in 2d/3d wire structures). Selected results for 100 μm thin NiTi wires demonstrate very large recoverable strains in combined tension-torsion, superelastic plateau type torque-twist angle responses and significant tension-torsion coupling characteristic for general load superelasticity.

Results of dynamic tensile tests performed on thin NiTi wires using a purposefully built vibration testing device for large frequencies ($<$ 100 Hz) and large strain amplitudes ($<$ 3%) show that the thermomechanical coupling effects due to periodical latent heat generation/absorption inherently accompanying the forward/reverse tensile superelastic cycling represent a significant factor limiting the superelastic damping applications to low frequencies and/or low strain amplitudes.

Support by EC via FP6 integrated projects AVALON (NMP2-CT-2005-515813) and UPWIND (019945 (SES6)) for this work is greatly acknowledged.

References

1. P. Sittner, V. Novák, L. Heller, P. Sedlák, M. Landa, J.V. Humbeeck, in *Proceedings of SMST* (Asilomar, California, USA) (in print)
2. A.R. Pelton, J. DiCello, S. Miyazaki, Min Invas Ther. Allied Technol. **9**, 107 (2000)
3. P. Sedlak, M. Frost (in preparation)
4. P. Sittner, L. Heller, A. Kujawa, M. Landa (in preparation)
5. V. Novák, P. Sittner, G.N. Dayananda, F.M. Braz-Fernandes, K.K. Mahesh, Mater. Sci. Eng. (in press)
6. P. Sittner, V. Novák, N. Zárubová, Acta Mater. **46**, 1265 (1998)
7. P. Sittner, Metall. Mater. Trans. **26A**, 2923 (1995)
8. J.V. Humbeeck, S. Kustov, Smart Mater. Struct. **14**, 171 (2005)
9. D.D.L. Chung, J. Mater. Sci. **8**, 5733 (2001)
10. A.M. Iadicola, A.J. Shaw, Int. J. Plast. **20**, 577 (2004)
11. E. Pieczyska, S. Gadaja, W.K. Nowackia, K. Hoshiob, Y. Makinob, H. Tobushi, Sci. Technol. Adv. Mater. **6**, 889 (2005)